Steering Matter Wave Superradiance with an Ultranarrow-Band Optical Cavity

H. Keßler, J. Klinder, M. Wolke, and A. Hemmerich*
Institut für Laser-Physik, Universität Hamburg, Luruper Chaussee 149, 22761 Hamburg, Germany
(Received 27 May 2014; published 12 August 2014)

A superfluid atomic gas is prepared inside an optical resonator with an ultranarrow bandwidth on the order of the single photon recoil energy. When a monochromatic off-resonant laser beam irradiates the atoms, above a critical intensity the cavity emits superradiant light pulses with a duration on the order of its photon storage time. The atoms are collectively scattered into coherent superpositions of discrete momentum states, which can be precisely controlled by adjusting the cavity resonance frequency. With appropriate pulse sequences the entire atomic sample can be collectively accelerated or decelerated by multiples of two recoil momenta. The instability boundary for the onset of matter wave superradiance is recorded and its main features are explained by a mean field model.

DOI: 10.1103/PhysRevLett.113.070404 PACS numbers: 03.75.-b, 34.50.-s, 42.50.Gy, 42.60.Lh

The coherent scattering of radiation by matter, commonly referred to as Rayleigh scattering, is a ubiquitous phenomenon in nature with basic consequences such as the blue color of the sky. If all scatterers are well localized within an optical wavelength of the incident radiation, their scattering contributions can sum up coherently, leading to a significant increase of the scattering cross section, a phenomenon closely related to the superradiance of collections of spontaneous emitters first discussed by Dicke [1–3]. Even, if the sample by far exceeds subwavelength dimensions, scattered photons can imprint spatial correlations into the matter sample, which strongly enhance phase coherent scattering into certain directions, similarly as in Bragg scattering from material lattice structures. The use of ultracold gases has permitted us to study superradiant Rayleigh scattering in the ultimate quantum mechanical limit when the atomic momentum is quantized in units of $\hbar k$ (with $k = 2\pi/\lambda$, $\lambda \equiv$ optical wavelength of the irradiated light), a regime that has been termed matter wave superradiance [4–7].

In the recent past remarkable progress has been made to tailor the light scattering properties of cold atomic matter ensembles in high finesse optical cavities [8]. This has lead to promising new cavity-aided laser cooling methods [9–13], the observation of collective atomic recoil lasing [14,15] and cavity enhanced Rayleigh scattering [16] in ring cavities, or to the realization of atom-cavity systems showing extreme nonlinear collective behavior, like optomechanical hysteresis and bistability [17,18] or self-organization instabilities [19–24]. In these experiments broadband cavities were used with linewidths well above the recoil frequency $\omega_{\mathrm{rec}} \equiv \hbar k^2/2m$ ($m =$ atomic mass) corresponding to the kinetic energy $E_{\mathrm{rec}} \equiv \hbar\omega_{\mathrm{rec}}$ gained by a resting atom after absorbing a single photon.

In this work we investigate matter wave superradiance of a Bose-Einstein condensate (BEC) of rubidium atoms in the presence of a narrow-band standing wave cavity, which combines subrecoil energy resolution with a Purcell factor far above unity [25,26], such that the electromagnetic vacuum is significantly modified [see Fig. 1(a)]. Such cavities have been recently shown to open up new regimes of cavity cooling and cavity optomechanics [27,28]. Here, we show that the use of such cavities in a Rayleigh scattering scenario, with a traveling pump wave irradiating the atoms perpendicularly with respect to the cavity axis, allows us to precisely address selected scattering channels, and thus to synthesize complex but yet well controlled, spatially periodic excited matter states preserving the full coherence of the initial condensate. We map out and explain the instability boundary for the onset of matter wave superradiance and discuss observations of suppression of superradiance, associated with destructive interference of different scattering channels. Remarkably, the

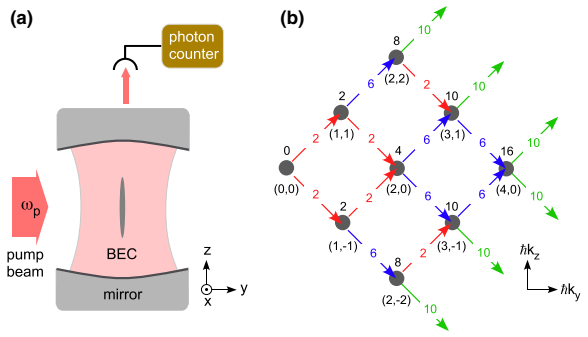

FIG. 1 (color online). (a) A pump beam with frequency ω_p impinges upon a BEC inside a high finesse resonator. (b) Relevant momentum states coupled to the BEC by scattering photons from the pump beam. The black tuples (n, m) below the filled gray disks denote the momenta of the respective momentum class along the y and z directions in units of $\hbar k$. The single numbers above the disks indicate the kinetic energy of the respective momentum class in units of the recoil energy. The colored numbers upon the arrows indicate the kinetic energy transfer associated with the respective scattering process.

single sided pumping of the atoms prevents the buildup of a stationary intracavity field even for negative detuning of the pump frequency with respect to the cavity resonance, in contrast to the observation of the Hepp-Lieb-Dicke phase transition [29] for standing wave pumping [22]. We use the cavity-aided control of Rayleigh scattering to demonstrate an efficient deceleration scheme for atoms, which could be also applied to other kinds of polarizable particles such as cold molecules.

In our experiment a cigar-shaped BEC of $N_a \approx 10^5$ ^{87}Rb atoms is held in a magnetic trap with trap frequencies $\Omega_{x,y,z}/2\pi = (215.6 \times 202.2 \times 25.2)$ Hz, irradiated by a pump beam propagating perpendicularly to the long axis of the condensate [see Fig. 1(a)]. The BEC with Thomas-Fermi radii (3.1,3.3,26.8) μm is prepared in the upper hyperfine component of the ground state $|F = 2, m_F = 2\rangle$. The single frequency ($\lambda = 803$ nm) pump beam with a radius $w_p = 80$ μm is far detuned from the relevant atomic resonances (the atomic $D_{1,2}$ lines at 795 and 780 nm), such that its interaction with the atoms is dispersive with negligible spontaneous emission. The new element in our work is a high finesse narrow-band optical cavity surrounding the BEC according to Fig. 1(a). The field decay rate of $\kappa = 2\pi \times 4.5$ kHz is smaller than $2\omega_{\rm rec} = 2\pi \times 7.1$ kHz, which corresponds to the kinetic energy $2E_{\rm rec}$ transferred to a resting atom by scattering a pump photon into the cavity. The cavity axis is well aligned with the weakly confined z axis of the condensate such that perfect spatial matching of the longitudinal transverse electromagnetic ($\rm TEM_{00}$) cavity mode with the atomic sample is obtained. The high finesse of the $\rm TEM_{00}$ mode ($\mathcal{F} = 3.44 \times 10^5$) together with its narrow beam waist ($w_0 \approx 31.2$ μm) yield a Purcell factor $\eta_c \approx 44$: i.e., the scattering into the $\rm TEM_{00}$ mode is enhanced by a factor of 44 with respect to scattering into all other modes of the radiation field [25,26]. Because of their preparation in the $|F = 2, m_F = 2\rangle$ hyperfine component of the ground state and the details of the $D_{1,2}$ lines, the maximal coupling to the atoms arises for left circularly polarized intracavity photons. For a uniform atomic sample, the $\rm TEM_{00}$ resonance frequency for left circularly polarized light is dispersively shifted by an amount $\delta_- = \frac{1}{2} N_a \Delta_-$ with an experimentally determined light shift per photon $\Delta_- = 2\pi \times 0.5$ Hz [30]. Hence, with $N_a = 10^5$ atoms $\delta_- = 2\pi \times 25$ kHz, which amounts to 5.6κ; i.e., the cavity operates in the regime of strong cooperative coupling.

As a consequence of the subrecoil bandwidth, cavity assisted scattering can only occur in a narrow resonance window such that only very few selected motional states are coupled. This is sketched in Fig. 1(b) for the simplified case when the transient formation of an intracavity optical lattice and the external trap are neglected and hence the atoms are considered as freely moving. Scattering of a pump photon by an atom in the BEC into the cavity corresponds to a transition from the $(0,0)\hbar k$ to the $(1,\pm1)\hbar k$ momentum states. Energy conservation requires $\omega_p - \omega_{\rm scat} = 2\omega_{\rm rec}$ with ω_p and $\omega_{\rm scat}$ denoting the pump frequency and the frequency of the scattered photon, respectively. The scattering process is best supported by the cavity if $\omega_{\rm scat}$ coincides with the effective cavity resonance frequency $\omega_{c,\rm eff} \equiv \omega_c - \delta_-$ with ω_c denoting the resonance frequency of the empty cavity; i.e., the effective detuning $\delta_{\rm eff} \equiv \omega_p - \omega_{\rm c,eff}$ should satisfy $\delta_{\rm eff} = 2\omega_{\rm rec}$. The same detuning allows us to resonantly scatter a second photon bringing the atom to the $(2,0)\hbar k$ state. Further scattering, which would transfer the entire atomic sample via the $(3,\pm1)\hbar k$ states to the $(4,0)\hbar k$ state, is not supported by the cavity unless $\delta_{\rm eff}$ is modified to account for the significantly larger energy costs of 6 recoil energies/atom. Because of the backaction of scattered photons upon the atomic sample, the scattering mechanism is expected to acquire collective character leading to the emission of a superradiant light pulse along the cavity axis: if the initial sample, a BEC in the $(0,0)\hbar k$ state, was perfectly homogeneous, scattering would be prevented by destructive interference from contributions from different locations within the BEC. Hence, quantum or thermal fluctuations are required to start the scattering process. Once a few photons are scattered into the cavity, the atoms transferred into the $(1,\pm1)\hbar k$ momentum states form a standing matter wave commensurate with the weak optical standing wave potential produced in the cavity. The matter wave grating acts as a Bragg grating, which enhances the scattering efficiency such that the optical standing wave and the corresponding matter grating grow in an exponential process reaching maximal values, when most atoms populate $(1,\pm1)\hbar k$. Their further transfer to $(2,0)\hbar k$ suppresses superradiance again, since in this state no density grating along the cavity axis is formed.

The onset of superradiant scattering above a characteristic intensity of the pump beam is observed in our experiment. In Fig. 2(a) we plot the intracavity power versus the frequency and the strength of the pump beam. The pump frequency is parametrized in terms of $\delta_{\rm eff}$ with $\delta_{\rm eff} = 0$ indicating the position of the cavity resonance in the presence of the BEC. The pump strength is specified in terms of the peak light shift ε_p caused by the pump beam in units of the recoil energy, which is spectroscopically measured [30]. To derive the plot in Fig. 2(a), the pump strength is increased linearly in time during 2 ms from 0 to $3E_{\rm rec}$ while the intracavity photon number is recorded by counting the photons leaking out through one of the mirrors. The observations show that at characteristic intensities, depending on $\delta_{\rm eff}$, short superradiant light pulses are emitted. The locations of their emergence in the $(\varepsilon_p, \delta_{\rm eff})$ plane take the approximate form of two nested parabolas rotated clockwise by 90°, which correspond to the instability boundaries for scattering associated with $2E_{\rm rec}$ and $6E_{\rm rec}$ kinetic energy transfer sketched by the red and blue arrows in Fig. 1(b). The exact locations of these boundaries depend on the time used to ramp up the pump

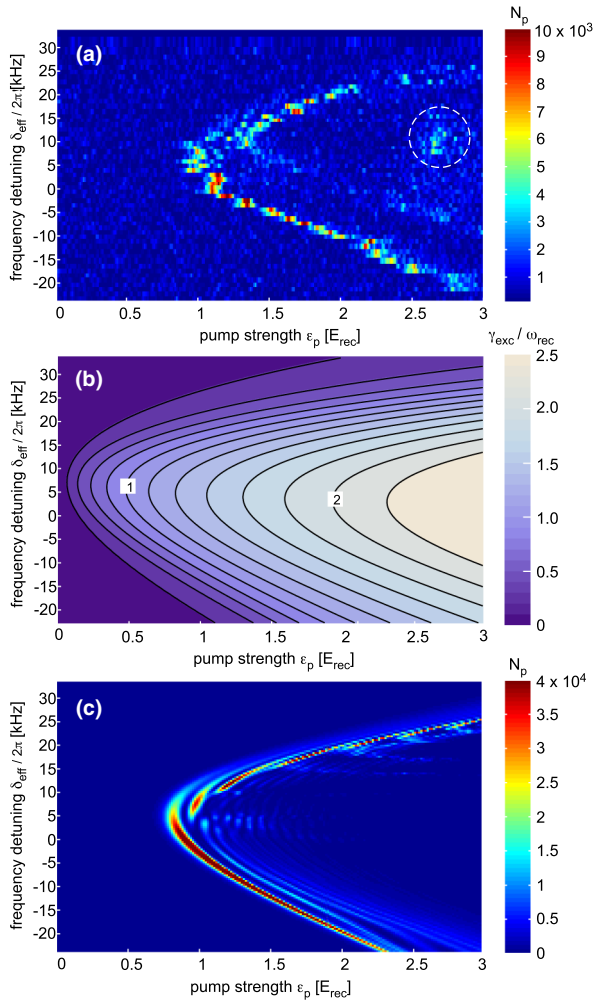

FIG. 2 (color online). (a) The intracavity photon number N_p is plotted versus the effective detuning $\delta_{\mathrm{eff}}/2\pi$ and the strength of the pump beam $\varepsilon_p/E_{\mathrm{rec}}$. The pump strength ε_p is linearly increased from 0 to $3E_{\mathrm{rec}}$ in 2 ms. As explained in the text, the signal within the dashed white circle is due to trap dynamics. (b) The excitation rate γ_{exc} characterizing the exponential instability is plotted versus $\delta_{\mathrm{eff}}/2\pi$ and $\varepsilon_p/E_{\mathrm{rec}}$. (c) Mean field simulation of the intracavity photon number for the pump strength ramp applied in (a).

power. In our experiment, we are limited to a few milliseconds by the trap oscillation time $T_y = 2\pi/\Omega_y \approx 5$ ms for the y direction. For ramping times approaching T_y the scattered atoms are decelerated at the trap edge and hence are tuned back into resonance. This effect is responsible for the revival of intracavity intensity within the dashed white circle in Fig. 2(a). The minimal pump strength required for superradiant scattering is found for $\delta_{\mathrm{eff}} \approx 2\omega_{\mathrm{rec}} = 2\pi \times 7.1$ kHz, which corresponds to the expected resonance condition for the $(0,0)\hbar k \rightarrow (1,\pm 1)\hbar k$ transitions.

The scattering instability can be understood by a simplified model only accounting for the $(0,0)\hbar k$ and $(\pm 1,\pm 1)\hbar k$ modes and neglecting depletion of the condensate [30]. This model possesses a steady state solution with zero intracavity intensity and all atoms in the BEC at $(0,0)\hbar k$. This solution is unstable in the entire $(\varepsilon_p, \delta_{\mathrm{eff}})$ plane with an exponential excitation rate $\gamma_{\mathrm{exc}}(\varepsilon_p, \delta_{\mathrm{eff}})$ plotted in Fig. 2(b). The graph shows that γ_{exc} is everywhere positive approaching zero on the δ_{eff} axis. The contours indicate trajectories of constant γ_{exc} specified in units of ω_{rec}. These trajectories reflect the form of the instability boundary found in the experiment [Fig. 2(a)]. In particular, the value of $\delta_{\mathrm{eff}} = 2\omega_{\mathrm{rec}}$, which minimizes ε_p along these trajectories agrees well with the observations. Note also the slight asymmetry with respect to the $\delta_{\mathrm{eff}} = 2\omega_{\mathrm{rec}}$ line, also observed in the experiment, which arises from contributions of the $(-1,\pm 1)\hbar k$ modes populated via rescattering of cavity photons into the pump mode (see the Supplemental Material [30]). A full mean field calculation of the intracavity photon number for the experimentally implemented 2 ms ramp of ε_p is shown in Fig. 2(c). The details of this calculation are deferred to the Supplemental Material [30]. The gross structure of the experimental data is nicely reproduced although the agreement is qualitative.

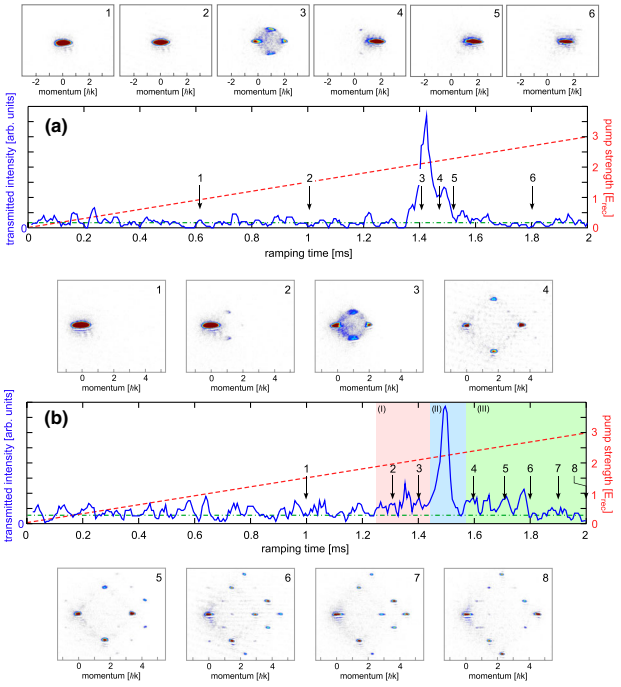

FIG. 3 (color online). The blue solid traces show the intensity leaking out of the cavity, while the pump strength is ramped [as in Fig. 2(a)] from 0 to $3E_{\mathrm{rec}}$ in 2 ms (as indicated by the red dashed traces) with negative detuning $\delta_{\mathrm{eff}}/2\pi = -12$ kHz in (a) and positive detuning $\delta_{\mathrm{eff}}/2\pi = 23$ kHz in (b), respectively. The insets numbered 1 to 6 in (a) and 1 to 8 in (b) show (single shot) momentum spectra taken at times marked by the black arrows. The green dashed dotted lines indicate the noise floor of the light detection. For momentum spectra taken at late times in the pump strength ramp, the higher order momentum components are decelerated at the trap edge, which explains the compression of these spectra along the horizontal axis.

In Fig. 3 we analyze the evolution of the momentum spectra of the atom sample corresponding to horizontal sections in Fig. 2(a) for negative [Fig. 3(a)] and positive [Fig. 3(b)] detunings $\delta_{\mathrm{eff}}/2\pi = -12$ kHz and $\delta_{\mathrm{eff}}/2\pi = 23$ kHz. In Fig. 3(a) the intracavity intensity displays a single sharp superradiant spike, during which the BEC is completely transferred to the $(2,0)\hbar k$ momentum state as is illustrated by the momentum spectra shown in the insets. Conservation of energy requires $\omega_{\mathrm{scat}} - \omega_p = 2\omega_{\mathrm{rec}}$. Hence, with $\delta_{\mathrm{eff}}/2\pi = -12$ kHz the frequency of the scattered light ω_{scat} deviates from the effective cavity resonance frequency $\omega_{c,\mathrm{eff}}$ by -4.3κ; i.e., the scattering processes $(0,0)\hbar k \rightarrow (1,\pm1)\hbar k \rightarrow (2,0)\hbar k$ [red arrows in Fig. 1(b)] are detuned from resonance. Other processes, however, are far more off resonant: for a subsequent transfer to $(4,0)\hbar k$, requiring $\omega_{\mathrm{scat}} - \omega_p = 6\omega_{\mathrm{rec}}$ [blue arrows in Fig. 1(b)], the detuning is $\omega_{\mathrm{scat}} - \omega_{c,\mathrm{eff}} = -7.5\kappa$. Hence, after complete transfer to $(2,0)\hbar k$, scattering is blocked although the pump strength is further increased.

The situation essentially changes, in the blue detuned case [Fig. 3(b)]. The values of $\omega_{\mathrm{scat}} - \omega_{c,\mathrm{eff}}$ for processes transferring $2E_{\mathrm{rec}}$, $6E_{\mathrm{rec}}$, or $10E_{\mathrm{rec}}$ to the atoms [cf. red, blue, and green arrows in Fig. 1(b)] are $(3.6, 0.37, -2.8)\kappa$. Hence, the transitions $(0,0)\hbar k \rightarrow (1,\pm1)\hbar k$ and $(1,\pm1)\hbar k \rightarrow (2,0)\hbar k$ with $2E_{\mathrm{rec}}$ energy transfer are significantly slower than the nearly resonant processes, connecting to the $(2,0)\hbar k$ and $(1,\pm1)\hbar k$ modes by transferring $6E_{\mathrm{rec}}$ to the atoms. Therefore, in the experiment, first an increase of the intracavity intensity is seen [region highlighted by red background in Fig. 3(b), indicated by (I)], which results from scattering atoms from the condensate mode $(0,0)\hbar k$ into the $(1,\pm1)\hbar k$ and $(2,0)\hbar k$ modes. Once these modes become populated, the much faster nearly resonant processes with $6E_{\mathrm{rec}}$ energy transfer set in [region highlighted in blue, (II)]. The resulting rapid depletion of the $(1,\pm1)\hbar k$ modes degrades the matter grating required to sustain the collective character of the $(0,0)\hbar k \rightarrow (2,0)\hbar k$ transition, which is therefore suppressed such that significant population can remain in the condensate mode as is seen in inset 4 of Fig. 3(b). This suppression of superradiant scattering is related to the mechanism of subradiance in the Dicke model of spontaneous emitters [3,36,37]. Finally, in the region highlighted in green and labeled (III), the comparatively weaker processes, associated with $10E_{\mathrm{rec}}$ energy transfer, populate an additional shell of momentum states, resulting in the small intracavity intensity level past $\approx$1.6 ms. The transfer of $14E_{\mathrm{rec}}$ would correspond to $\omega_{\mathrm{scat}} - \omega_{c,\mathrm{eff}} = -6\kappa$, with the consequence that such processes are practically suppressed. As the insets in Fig. 3(b) show, only momentum states $(n,m)\hbar k$ become populated, which require at most $10E_{\mathrm{rec}}$ kinetic energy transfer per scattering event, i.e., $0 \le n \le 6, -3 \le m \le 3$ with the constraint $n + |m| \le 6$.

Our findings demonstrate a new regime of control of matter wave superradiance in optical cavities. This may, for example, be used to decelerate an initially moving BEC by a series of pump pulses with appropriately adjusted frequencies and intensities. In Fig. 4 a BEC, initially prepared in the $(-4,0)\hbar k$ momentum state, is decelerated by two successive pump pulses: a first 350 μs long pulse with $\delta_{\mathrm{eff}}/2\pi = -31$ kHz, $\varepsilon_p = 2.5E_{\mathrm{rec}}$ followed by a second pulse with $\delta_{\mathrm{eff}}/2\pi = -16$ kHz, $\varepsilon_p = 2.9E_{\mathrm{rec}}$ and 160 μs duration. The insets depicting momentum spectra at different times during the pulse sequence show that the initial BEC after 0.5 ms is transferred to zero momentum. Note that due to collisions a significant amount of atoms is dispersed among a continuum of scattering states leading to the diffuse gray background. By adding additional pulses this scheme may be readily extended for deceleration of much faster particle samples. Other pulse sequences may be designed to implement efficient matter wave beam splitters or multiple path matter wave interferometers. An interesting future perspective of our work is the search for quantum entanglement between light and matter observables [38].

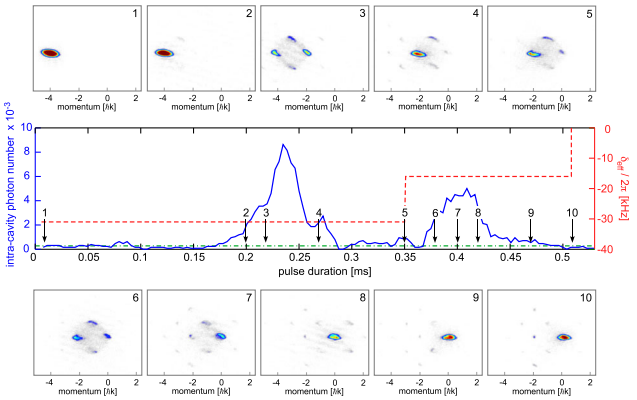

FIG. 4 (color online). The blue solid traces shows the intracavity intensity for a sequence of two pump pulses with 350 and 160 μs durations and detunings $\delta_{\mathrm{eff}}/2\pi = -31$ kHz and $\delta_{\mathrm{eff}}/2\pi = -16$ kHz as indicated by the red dashed line. The pump strength was $\varepsilon_p = 2.5E_{\mathrm{rec}}$ and $\varepsilon_p = 2.9E_{\mathrm{rec}}$, respectively. The insets show momentum spectra at different times indicated by black arrows.

This work was partially supported by DFG-SFB 925 and DFG-GrK1355. We are grateful to Michael Thorwart, Reza Bakhtiari, Duncan O'Dell, and Helmut Ritsch for useful discussions. We also thank Claus Zimmermann for his constructive critical reading of the manuscript.

*hemmerich@physnet.uni-hamburg.de

[1] R. H. Dicke, Phys. Rev. **93**, 99 (1954).
[2] R. H. Dicke, in *Proceedings of the Third International Congress on Quantum Electronics*, edited by P. Grivet and N. Bloembergen (Columbia University Press, New York, 1964), pp. 35–54.
[3] M. Gross and S. Haroche, Phys. Rep. **93**, 301 (1982).

[4] S. Inouye, A. P. Chikkatur, D. M. Stamper-Kurn, J. Stenger, D. E. Pritchard, and W. Ketterle, Science **285**, 571 (1999).
[5] Y. Yoshikawa, T. Sugiura, Y. Torii, and T. Kuga, Phys. Rev. A **69**, 041603(R) (2004).
[6] N. Bar-Gill, E. E. Rowen, and N. Davidson, Phys. Rev. A **76**, 043603 (2007).
[7] A. Hilliard, F. Kaminski, R. le Targat, C. Olausson, E. Polzik, and J. Müller, Phys. Rev. A **78**, 051403(R) (2008).
[8] H. Ritsch, P. Domokos, F. Brennecke, and T. Esslinger, Rev. Mod. Phys. **85**, 553 (2013).
[9] P. Horak, G. Hechenblaikner, K. M. Gheri, H. Stecher, and H. Ritsch, Phys. Rev. Lett. **79**, 4974 (1997).
[10] V. Vuletić and S. Chu, Phys. Rev. Lett. **84**, 3787 (2000).
[11] P. Maunz, T. Puppe, I. Schuster, N. Syassen, P. W. H. Pinkse, and G. Rempe, Nature (London) **428**, 50 (2004).
[12] A. Beige, P. L. Knight, and G. Vitiello, New J. Phys. **7**, 96 (2005).
[13] G. Morigi, P. W. H. Pinkse, M. Kowalewski, and R. de Vivie-Riedle, Phys. Rev. Lett. **99**, 073001 (2007).
[14] D. Kruse, C. von Cube, C. Zimmermann, and Ph. W. Courteille, Phys. Rev. Lett. **91**, 183601 (2003).
[15] S. Slama, S. Bux, G. Krenz, C. Zimmermann, and Ph. W. Courteille, Phys. Rev. Lett. **98**, 053603 (2007).
[16] S. Bux, C. Gnahm, R. A. W. Maier, C. Zimmermann, and P. W. Courteille, Phys. Rev. Lett. **106**, 203601 (2011).
[17] F. Brennecke, S. Ritter, T. Donner, and T. Esslinger, Science **322**, 235 (2008).
[18] T. P. Purdy, D. W. C. Brooks, T. Botter, N. Brahms, Z.-Y. Ma, and D. M. Stamper-Kurn, Phys. Rev. Lett. **105**, 133602 (2010).
[19] P. Domokos and H. Ritsch, Phys. Rev. Lett. **89**, 253003 (2002).
[20] H. W. Chan, A. T. Black, and V. Vuletić, Phys. Rev. Lett. **90**, 063003 (2003).
[21] A. T. Black, H. W. Chan, and V. Vuletić, Phys. Rev. Lett. **91**, 203001 (2003).
[22] K. Baumann, C. Guerlin, F. Brennecke, and T. Esslinger, Nature (London) **464**, 1301 (2010).
[23] K. J. Arnold, M. P. Baden, and M. D. Barrett, Phys. Rev. Lett. **109**, 153002 (2012).
[24] D. Schmidt, H. Tomczyk, S. Slama, and C. Zimmermann, Phys. Rev. Lett. **112**, 115302 (2014).
[25] E. M. Purcell, H. C. Torrey, and R. V. Pound, Phys. Rev. **69**, 37 (1946).
[26] H. Tanji-Suzukia *et al.*, *Advances in Atomic, Molecular, and Optical Physics* (Elsevier, New York, 2011), Vol. 60.
[27] M. Wolke, J. Klinner, H. Keßler, and A. Hemmerich, Science **337**, 75 (2012).
[28] H. Keßler, J. Klinder, M. Wolke, and A. Hemmerich, New J. Phys. **16**, 053008 (2014).
[29] K. Hepp and E. H. Lieb, Ann. Phys. (N.Y.) **76**, 360 (1973).
[30] See Supplemental Material http://link.aps.org/supplemental/10.1103/PhysRevLett.113.070404, which includes Refs. [31–35], more detailed information on experimental protocols, and an outline of the mean field calculation at the basis of the plots shown in Figs. 2(b) and (c) of the main text.
[31] D. Hansen and A. Hemmerich, Phys. Rev. Lett. **96**, 073003 (2006).
[32] J. Klinner, M. Wolke, and A. Hemmerich, Phys. Rev. A **81**, 043414 (2010).
[33] T. Esslinger, I. Bloch, and T. W. Hänsch, Phys. Rev. A **58**, R2664 (1998).
[34] C. M. Bender and S. Boettcher, Phys. Rev. Lett. **80**, 5243 (1998).
[35] R. Bachelard, H. Bender, Ph. W. Courteille, N. Piovella, C. Stehle, C. Zimmermann, and S. Slama, Phys. Rev. A **86**, 043605 (2012).
[36] R. G. DeVoe and R. G. Brewer, Phys. Rev. Lett. **76**, 2049 (1996).
[37] M. M. Cola, D. Bigerni, and N. Piovella, Phys. Rev. A **79**, 053622 (2009).
[38] W. Niedenzu, R. M. Sandner, C. Genes, and H. Ritsch, J. Phys. B **45**, 245501 (2012).